

AUTONOMOUS TOPOGRAPHY DETECTION AND TRAVERSAL FOR AN INSPECTION ROBOT WITHIN THE BEAMLINER OF PARTICLE ACCELERATORS

N. Schweizer*, RMR, Technische Universität Darmstadt, Germany

I. Pongrac, GSI Helmholtzzentrum für Schwerionenforschung GmbH, Darmstadt, Germany

Abstract

Particle accelerators feature ultra-high vacuum pipe systems with unique topography, i.e. with a multitude of different vacuum chambers of varying dimensions and varying pipe apertures. In order to be able to examine the interior of the entire vacuum system, even those parts which are not accessible without disassembling large parts of the accelerator, a semi-autonomous robot is being developed which shall traverse and visually inspect the vacuum system of particle accelerators. We present a generic concept based on distance sensors for the inspection robot to detect steps between vacuum chambers and gaps in the beamline. Movement strategies to autonomously overcome these basic obstacles are introduced. For evaluation we use simulations of ideal environments with flat surfaces as well as realistic beam pipe environments of the SIS100 particle accelerator. Additionally, a prototype of our robot concept confirms the implementation of all maneuvers. Results show that obstacles of previously unknown dimensions can be detected and reliably traversed.

INTRODUCTION

Inspecting the ultra-high vacuum beamline system of a particle accelerator visually can be essential to examine the system's integrity. Forgotten tools, e.g. after maintenance work, damaged components or any foreign objects might impair the beam quality and even inhibit beam experiments. For the heavy ion synchrotron SIS100 of the international accelerator facility FAIR [1], which is currently under construction at the premises of GSI in Darmstadt, Germany, an inspection robot is being developed [2]. A modular design enables the robot to traverse the unique and challenging topography of varying vacuum chambers. At the connection of two different pipe sections one or several steps occur where the robot has to climb up or down. Additionally, pump chambers as well as for instance kicker and septa tanks have deep gaps which have to be overcome directly.

The actual robot prototype, shown in Fig. 1, consists of four wheeled modules connected via pitch rotational joints and is able to traverse single steps and gaps. It can be manually controlled to climb up or down and to safely reach the other side of a gap. However, within the vacuum system the robot cannot be observed visually. Thus, these obstacles should be detected and traversed autonomously. In the following, a sensor configuration is described to detect and distinguish different obstacles. Afterwards, autonomous

driving maneuvers for overcoming steps and gaps are discussed.



Figure 1: Prototype of the modular in-pipe inspection robot with 3D printed frames and wheels.

SENSOR ARRANGEMENT

For autonomous locomotion the robot has to recognize all obstacles, continuously monitoring its environment. During climbing maneuvers, almost each movement step depends on a sensor feedback that shows the achievement of a specific position. Therefore, multiple distance sensors are required. In Fig. 2 scanning beams of the sensors are visualized. One is mounted on the front side in the center of the robot to detect steps to a higher ground level. An additional distance sensor, centered and directed downwards, is positioned behind the first wheel pair. By evaluating this sensor, the transition to pipes with larger diameters and therefore downward steps or gaps can be detected. In order to decide whether the robot has to traverse a downward step on the one hand or a deep gap on the other hand, a measured depth larger than 100 mm is defined as a gap. This value is determined by practical considerations of the vacuum pipe system of SIS100, but can of course be adapted to other pipe topographies.



Figure 2: Sensor arrangement of the inspection robot indicated by the corresponding scanning beam directions.

Further sensors are mounted beneath the first and the last joint axles and at the rear side behind the last wheels. With respect to the symmetrical design and in order to have the possibility of driving forwards as well as backwards, an additional sensor is placed on the rear side of the robot. All inner sensors are directed downwards, only the front and the back sensors are directed in longitudinal direction of the beam pipe. In total, the robot is equipped with six distance sensors in its configuration of four modules; accordingly,

* nicolai.schweizer@rnr.tu-darmstadt.de

Content from this work may be used under the terms of the CC BY 3.0 licence (© 2018). Any distribution of this work must maintain attribution to the author(s), title of the work, publisher, and DOI.

more distance sensors are needed in case of configurations of more than four modules.

MANEUVER BEHAVIOR

Climbing Up

As soon as a stair is in the range of the front sensor, the maneuver for climbing up is initiated and lets the robot stop approximately 20 mm in front of the obstacle. The distance z_g between the lowest wheel point and the pipe's ground level measured by the sensor behind the wheels gives the current pipe radius

$$r_p = \frac{z_g^2 + y_w^2}{2z_g}, \quad (1)$$

with y_w as the half track width of the robot, see Fig. 3, and $z_g > 0$. A measurement of $z_g = 0$ implies that the robot is located on a flat surface as it is shown in Fig. 4.

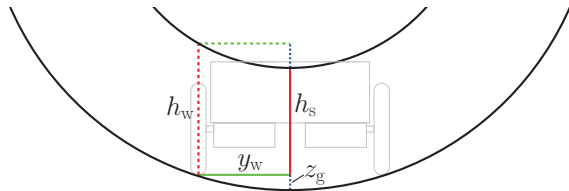


Figure 3: The measured step height h_s between two pipes is smaller than the necessary lifting height for the wheels h_w .

Next, the stair height has to be determined. Therefore, the front module is repeatedly lifted and a new distance is measured by the front sensor after each lifting step. By comparing the last two measurements, the edge of the stair can be recognized. As soon as the scanning beam of the sensor is directed slightly above the edge of the step, see Fig. 4b), the scanning range increases abruptly by at least several centimeters, so that the lifting sequence is stopped. With the actual angle ϕ_1 of the first joint and the initial distance to the stair $x_{\phi_1=0}$ the step height h_s can be calculated as

$$h_s = z_j + (l_{m1} + x_{\phi_1=0}) \cdot \tan \phi_1. \quad (2)$$

Here, z_j describes the height of the joint axle and the front sensor relative to a flat surface through the lowest wheel points as illustrated in Fig. 5. l_{m1} denotes the module length measured from the joint to the sensor position. From Fig. 3

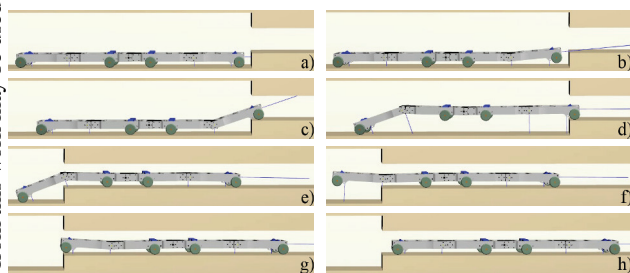


Figure 4: Movement steps of a climbing up maneuver.

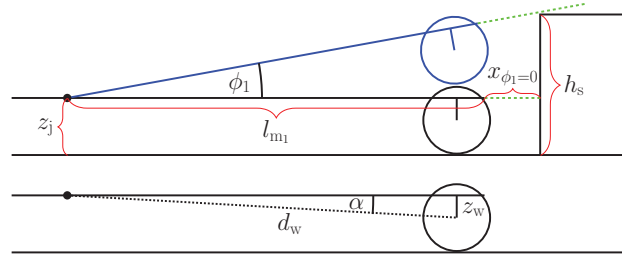


Figure 5: Front module of the robot and relevant parameters for stair height measurement h_s . In blue, the module has been already lifted. The green dashed lines show the scanning beam of the sensor.

can be obtained that in pipe environments the actual step height h_w is larger since the vertical distance between the two pipe surfaces increasingly becomes larger to the sides of the pipes:

$$h_w = r_p - z_g - \sqrt{(r_p - h_s - z_g)^2 - y_w^2}. \quad (3)$$

This height leads to the required joint angle

$$\phi_1(h_w) = \alpha + \arcsin\left(\frac{h_w - z_w}{d_w}\right), \quad (4)$$

where z_w denotes the vertical distance between the wheel axle and the joint and d_w its absolute distance. The angle between the horizontal from the joint and the wheel axle is described by α as illustrated in Fig. 5.

Next, the first module is lifted by angle ϕ_1 determined from (4) and the robot drives forward until the first wheel pair is above the higher step surface recognized by the sensor which is mounted behind the front wheels scanning downwards. Then, in Fig. 4d) the second and the third module are aligned with the first one while they are lifted to the new height level. During this movement the last module has to compensate the height difference

$$\Delta z_{j1}(\phi_1) = h_w - z_w - \sin(\phi_1 - \alpha) \cdot d_w \quad (5)$$

between the lifted axles of the joints and their initial position above the lower pipe surface z_j . The corresponding angle of the last joint is given by

$$\phi_3(\Delta z_{j1}) = -\alpha + \arcsin\left(\frac{\Delta z_{j1} + z_w}{d_w}\right). \quad (6)$$

Subsequently, the robot moves forward until the sensor beneath the last joint indicates in Fig. 4e) that the higher step surface is reached. To prevent a collision with the stair edge, which could occur due to mechanical compliances, the last module is now lifted slightly higher instead of aligning with the other modules. For the last movement step a short time-dependent sequence is added. While moving forward again, the sensor in front of the last wheel pair will detect the stair edge, and the robot has to move a bit further in order to bring its rear wheels onto the step of the new pipe section. Finally, in Fig. 4h) the last module is lowered and aligned with the rest of the robot.

Climbing Down

Once the robot has detected a downward step, it keeps moving forward until the first joint has passed the stair edge which is identified by its corresponding sensor. Before lowering the first module, the heights h_s and h_w have to be determined. By using the sensor at the joint instead of the one at the front wheels, the measurement is more precise because of reduced influence of mechanical compliances caused by gravitational forces. From the measured distance d_m , sketched in Fig. 6, the stair height of flat surfaces can be determined by

$$h_s = d_m - z_j + z_s, \quad (7)$$

with z_s denoting the distance from the sensor to the joint axle. For a pipe environment the total height is

$$h_w = z_g - r_p + \sqrt{(r_p + h_s - z_g)^2 - y_w^2}, \quad (8)$$

where r_p , determined by (1), and z_g are now referred to the smaller pipe. The required inclination angle for the front module follows from (6), identifying $\phi_3 = \phi_1$ and $\Delta z_{j_1} = h_w$.

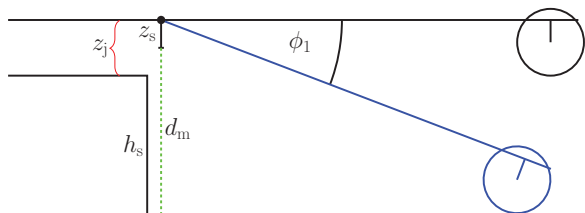


Figure 6: Relevant parameters for stair height measurement. Displayed is the front module of the robot that has been already moved over the edge of the step. In blue, the module has been lowered by an angle of ϕ_1 to reach the lower surface.

After the module is lowered, the robot moves forward and stops again as soon as the sensor next to the last wheel pair reaches the larger pipe diameter. The rear wheels are now located closely to the stair edge, but still on the higher pipe level. Similar to the climbing up maneuver, in the next motion sequence the first module will be aligned horizontally. In parallel, the last module will compensate the height difference

$$\Delta z_{j_1}(\phi_1) = h_w + z_w - \sin(\phi_1 + \alpha) \cdot d_w \quad (9)$$

measured from the initial joint position on the higher pipe level. By identifying $\phi_1 = \phi_3$ and $h_w = \Delta z_{j_1}$, (4) yields the actual angle of the last joint. Eventually, modules one to three have ground contact on the lower pipe surface.

Before the last module can be aligned to conclude the maneuver, the robot has to move forward for a small distance so that the rear wheels can be lowered without any collision with the pipe wall.

Crossing a Gap

If a gap is detected, the robot will be stopped as displayed in Fig. 7a). Then, the first module is raised slightly in order

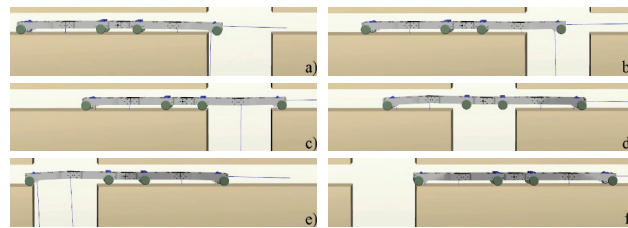


Figure 7: Movement steps for crossing a gap.

to prevent a collision of the wheels with the edge on the other side of the gap due to mechanical compliance, see Fig. 7b). The robot moves forward until it reaches the other edge of the gap which will be indicated by the corresponding wheel sensor. In Fig. 7c) three wheel pairs are located in front of the gap and the front wheel pair is slightly above ground level behind the gap. The front module will be lowered until the wheels touch the surface of the pipe. Moreover, the two outer joints are lifted slightly by giving a small inclination angle to the outer modules to hold the inner modules a little above the pipe surface. While moving forward in Fig. 7d), this avoids a collision of the inner wheels with the edge of the gap. The robot will be stopped again as soon as the sensor at the last wheels detects the gap, see Fig. 7e). Now, the first and last modules will be aligned horizontally so that the inner wheels touch the ground. Thereafter, the last module is slightly raised so that it loses contact with the pipe surface in front of the gap. Moving forward until the last wheel pair is on the other side of the gap and lowering the rear module will conclude the crossing gap maneuver in Fig. 7f).

CONCLUSION

A sensor-based concept for an inspection robot to detect and traverse basic topographic structures within the beamline of particle accelerators was introduced. 3D robotic simulations with flat surfaces and with CAD models of the SIS100 showed successful obstacle detection. Collision-free movement sequences confirmed the feasibility of the described maneuvers. Moreover, if the narrower pipe has an elliptical shape, as is the case for SIS100 dipole and quadrupole chambers, the climbing tasks were also performed successfully. In such scenarios the calculated lifting height is a bit larger than necessary. However, a slightly higher lifting or lowering of the modules can be accepted and still leads to successful traversing. This was also proven in experiments with our prototype device, which indicated some inaccuracies of the stair height measurement due to the conical view of the distance sensor. In future, more complex topographies like double steps or a step followed by a gap will be considered.

REFERENCES

- [1] P. Spiller and G. Franchetti, "The FAIR accelerator project at GSI", in *Nucl. Instrum. Meth. A*, 561 (2), pp. 305–309, 2006.
- [2] N. Schweizer and I. Pongrac, "Semi-autonomous device for visual inspection of vacuum beamlines of particle accelerators", in *Proc. IPAC'17*, Copenhagen, Denmark, May 2017, paper THPVA042, pp. 4528–4530.